Electronic Supplementary Information for

Highly Lubricative, Self-Healing, Chemically Degradable, Anti-Flaming and Anti-Irradiating Magnetic Gels Simply from Binary Mixtures of Fe_3O_4 Nanoparticles and Water

Lulin Hu,[†, ‡] Weiyan Yu,[†, ‡] Jian Liu,[†] Yi Yang,[†, ‡,] Jingcheng Hao[‡,§] and Lu Xu[†, ‡,*]*

[†]*State Key Laboratory of Solid Lubrication, Lanzhou Institute of Chemical Physics, Chinese Academy of Sciences, Lanzhou 730000, People's Republic of China;*

[‡]*Shandong Laboratory of Advanced Materials and Green Manufacturing at Yantai, Yantai 264000, People's Republic of China;*

[§]*Key Laboratory of Colloid and Interface Chemistry & Key Laboratory of Special Aggregated Materials, Shandong University, Jinan 250100, People's Republic of China.*

Corresponding authors: yangyi@licp.cas.cn; xulu@licp.cas.cn

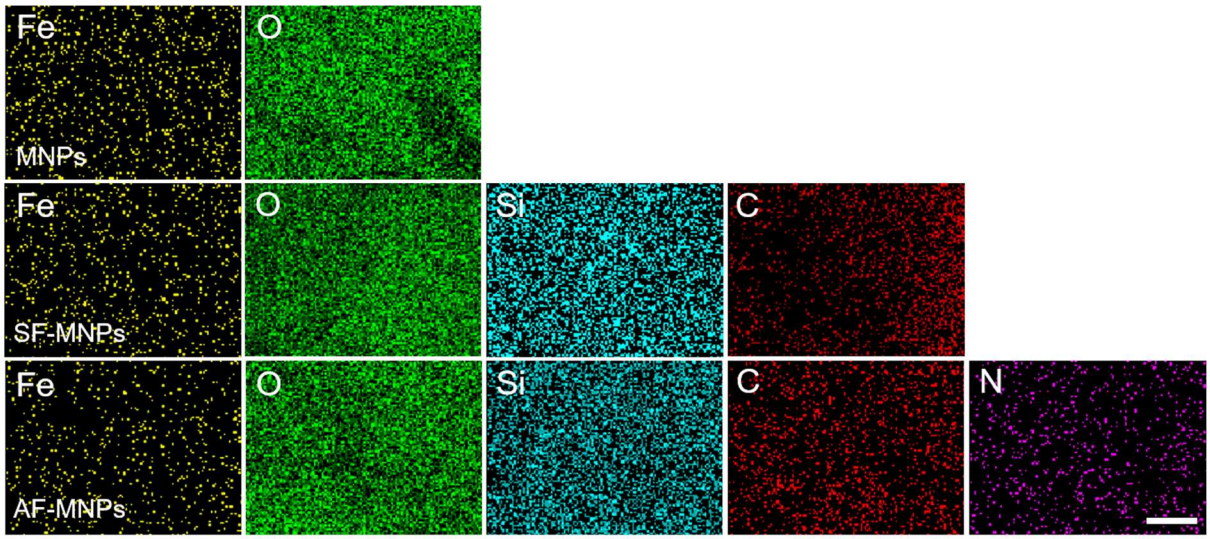

Figure S1. Element distribution on the surface of pristine, SF-, and AF-MNPs. Scale bar = 1 μm.

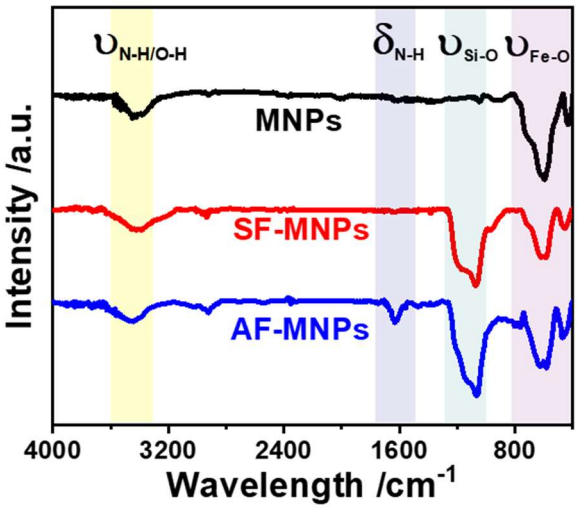

Figure S2. FT-IR spectra of pristine, SF- and AF-MNPs. T = 25 °C.

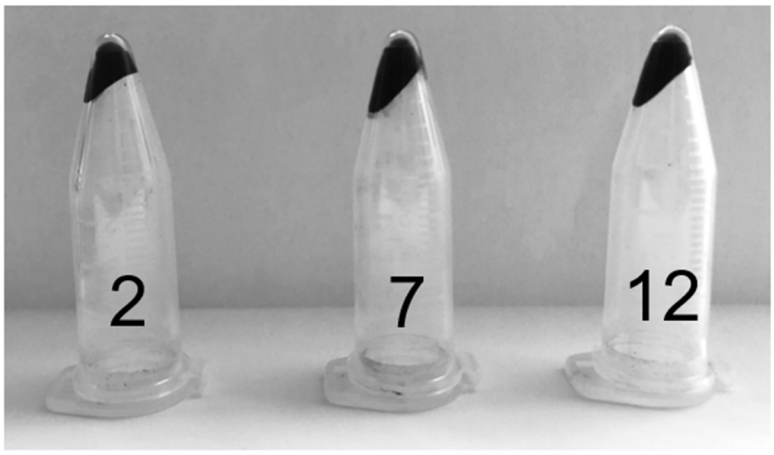

Figure S3. Photographs of the inorganic Fe_3O_4 gels. The numbers refer to the internal pH values of the aqueous gels. T = 25 °C.

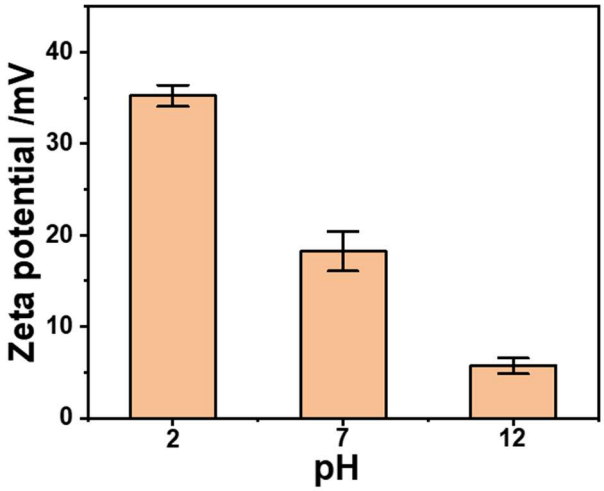

Figure S4. Zeta potential measurements of 1 mg mL^{-1} aqueous suspensions of AF-MNPs at different pH values. T = 25 °C. c_{Fe3O4} = 48 wt%.

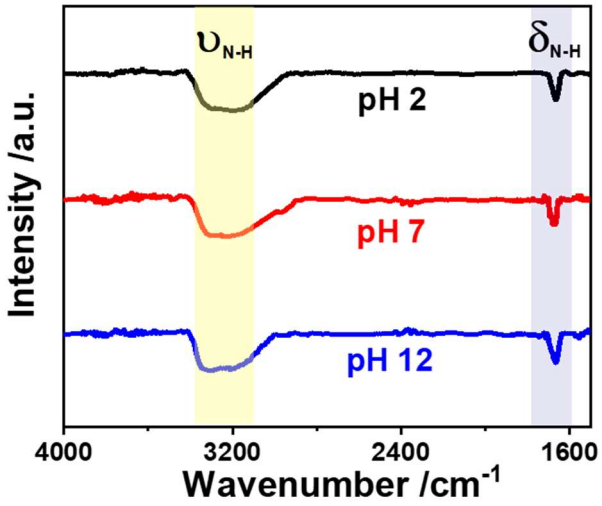

Figure S5. FT-IR spectra of lyophilized Fe_3O_4 gels at pH 2, 7 and 12, respectively. T = 25 °C. c_{Fe3O4} = 48 wt%.

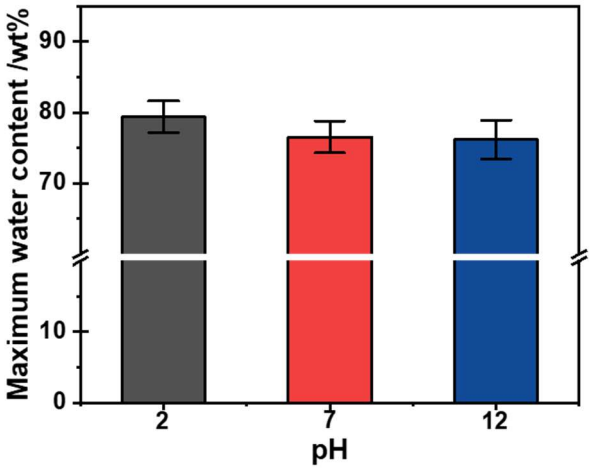

Figure S6. Maximum water content (in wt%) of the magnetic gels with different internal pH values. T = 25 °C.

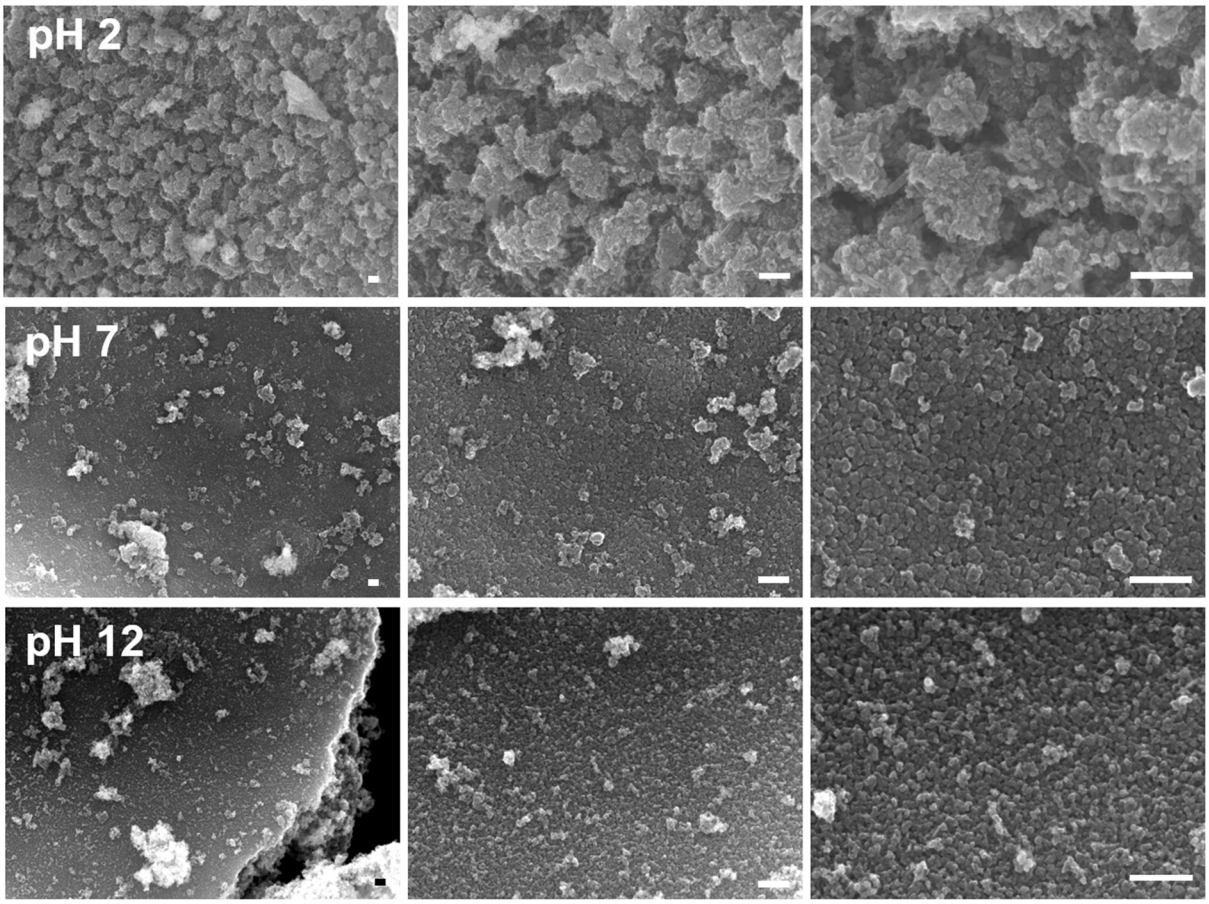

Figure S7. SEM images of freeze-dried Fe_3O_4 gels obtained at different scanning locations and magnifications. Scale bar = 100 nm. c_{Fe3O4} = 48 wt%.

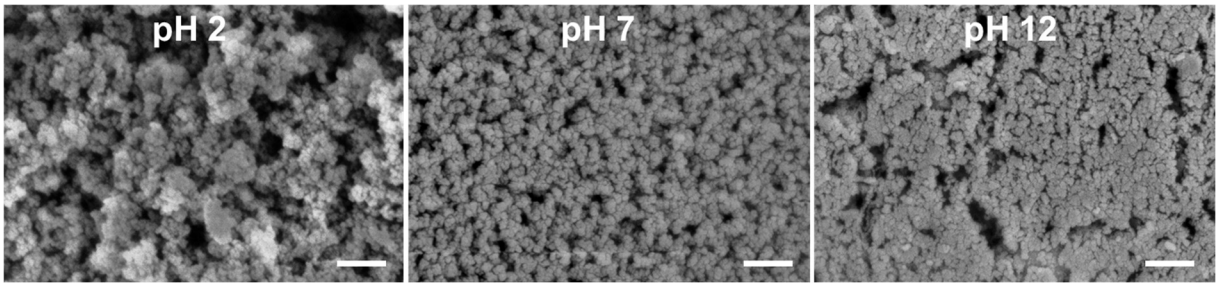

Figure S8. Cryogenic scanning electron microscopy (cryo-SEM) observations of the Fe_3O_4 gels at pH 2, 7 and 12, respectively. Scale bar = 100 nm. c_{Fe3O4} = 48 wt%.

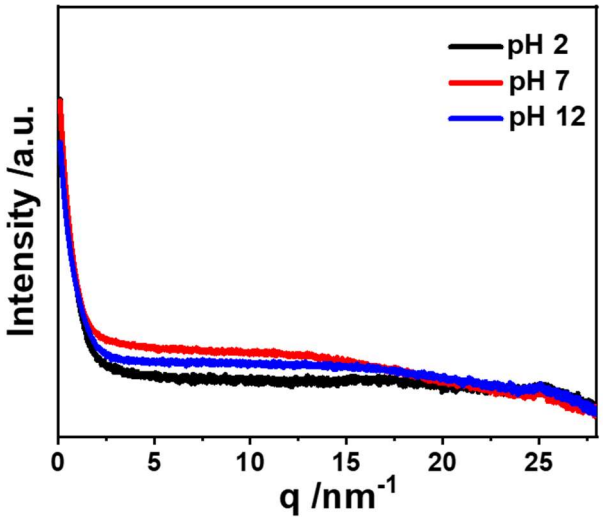

Figure S9. SAXS patterns of lyophilized Fe_3O_4 gels at different pH values. T = 25 °C. c_{Fe3O4} = 48 wt%.

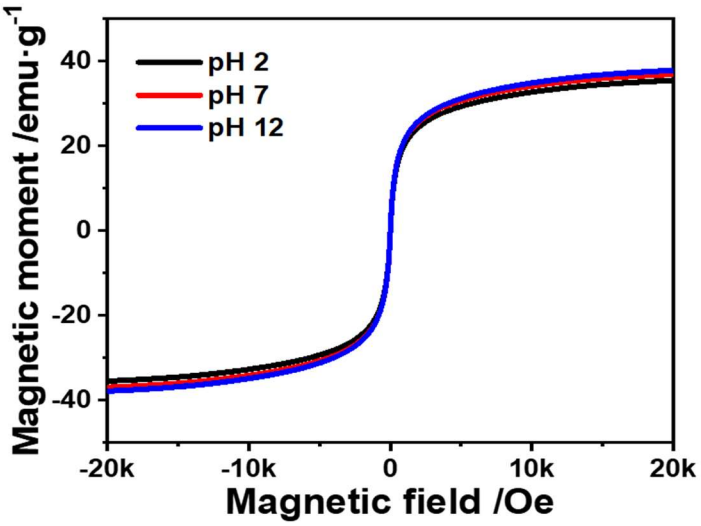

Figure S10. SQUID magnetometry profiles of 48 wt% Fe_3O_4 gels with different internal pH values at 25 °C.

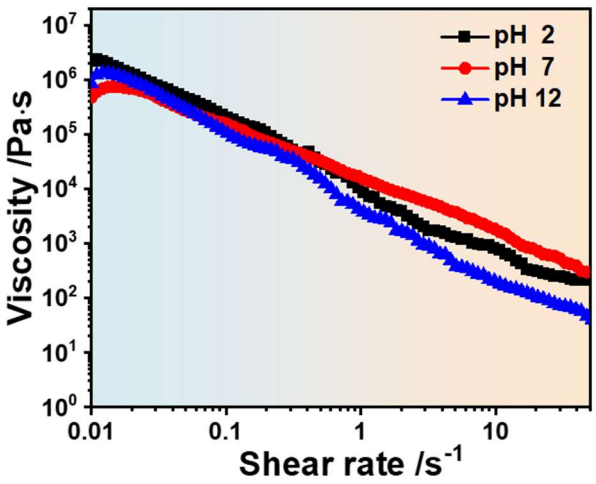

Figure S11. Colloidal viscosity of the Fe_3O_4 gels at shear rates between 0.01 and 50 s^{-1}. T = 25 °C. c_{Fe3O4} = 48 wt%.

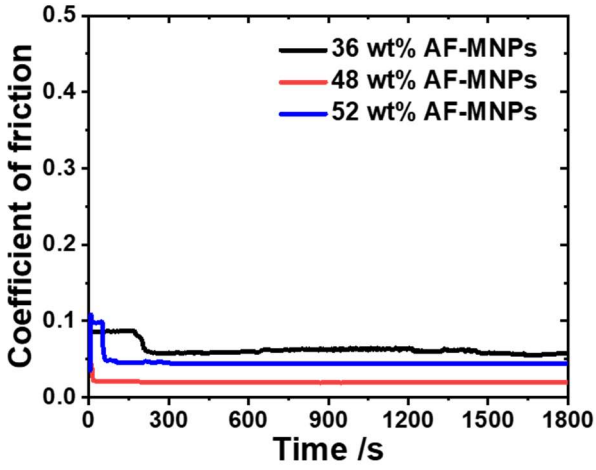

Figure S12. Effect of particle concentration on the CoF of pH 12 Fe_3O_4 gels at 800 N and 20 Hz. T = 25 °C.

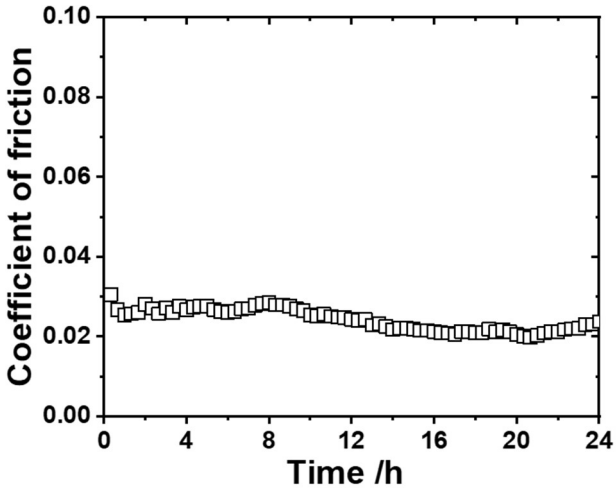

Figure S13. CoF of the pH 12 Fe_3O_4 gel upon continuously used for 24 h under 800 N and 20 Hz. T = 25 °C. c_{Fe3O4} = 48 wt%.

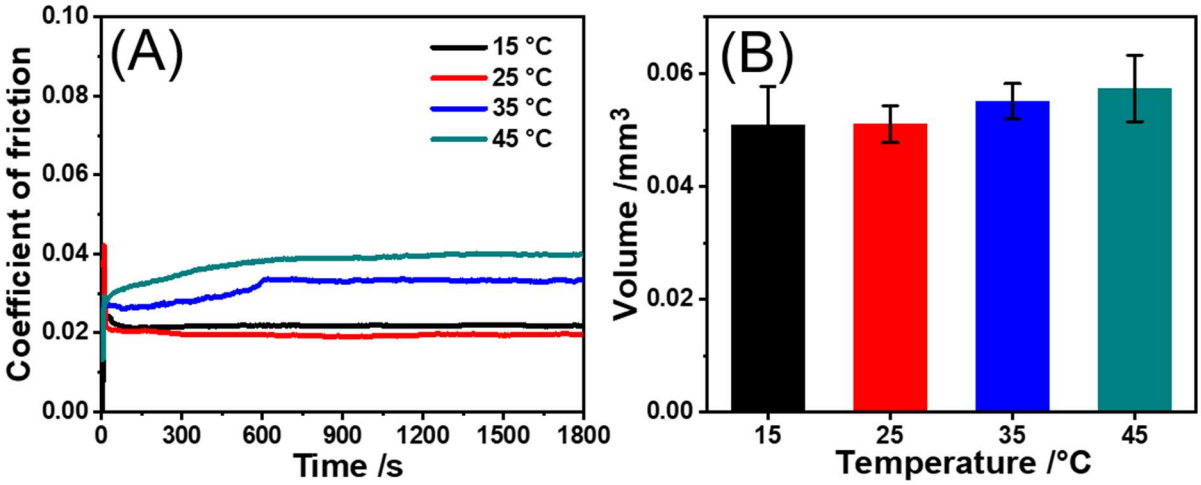

Figure S14. (A) CoF and (B) wear volume of the pH 12 Fe_3O_4 gel at temperatures between 15 and 45 °C under 800 N and 20 Hz. c_{Fe3O4} = 48 wt%.

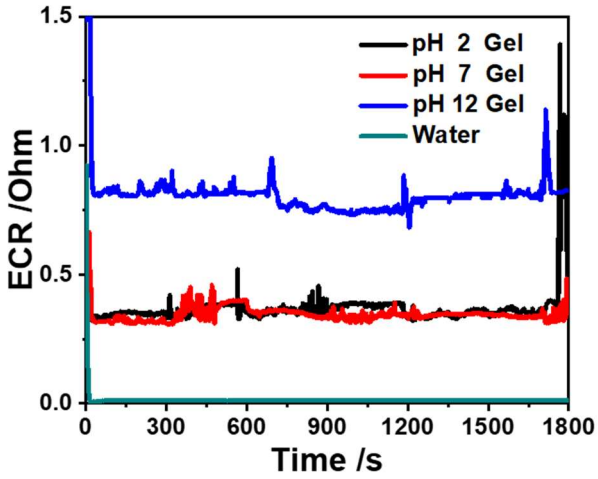

Figure S15. ECR of water and Fe_3O_4 gels with different internal pH values at 25 °C. c_{Fe3O4} = 48 wt%.

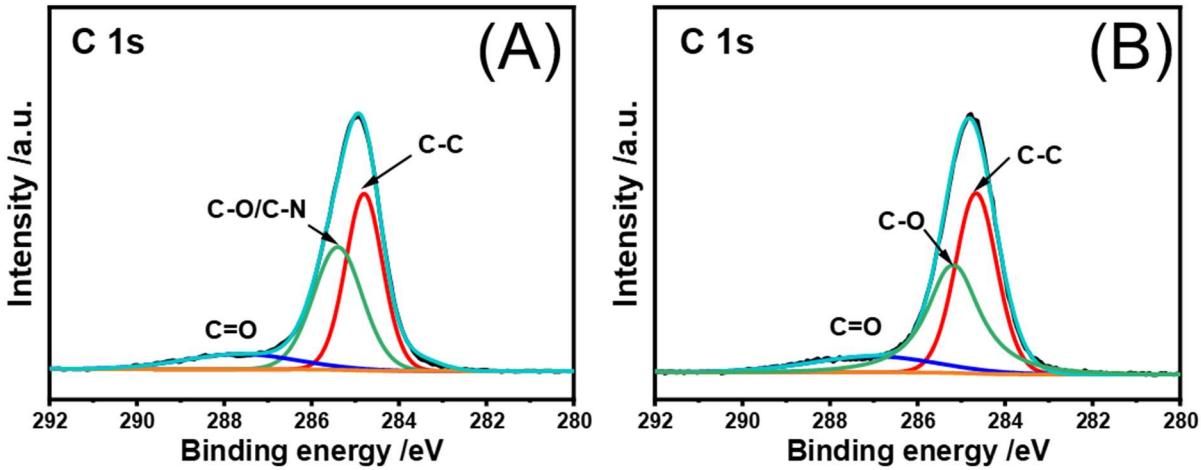

Figure S16. XPS C 1s spectra of steel substrates lubricated with (A) pH 12 Fe_3O_4 gel and (B) ultrapure water, respectively. T = 25 °C.

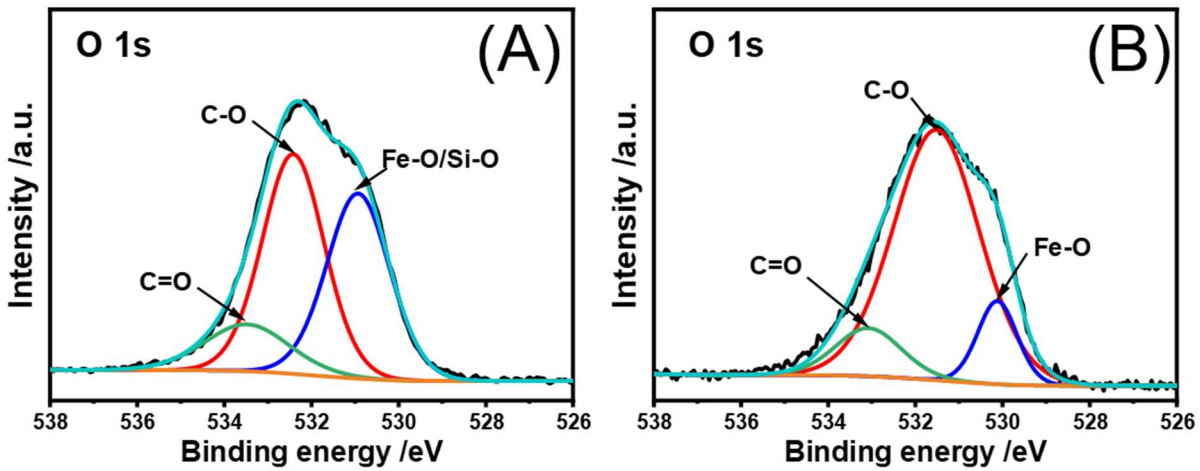

Figure S17. XPS O 1s spectra of steel substrates lubricated with (A) pH 12 Fe_3O_4 gel and (B) deionized water, respectively. T = 25 °C.

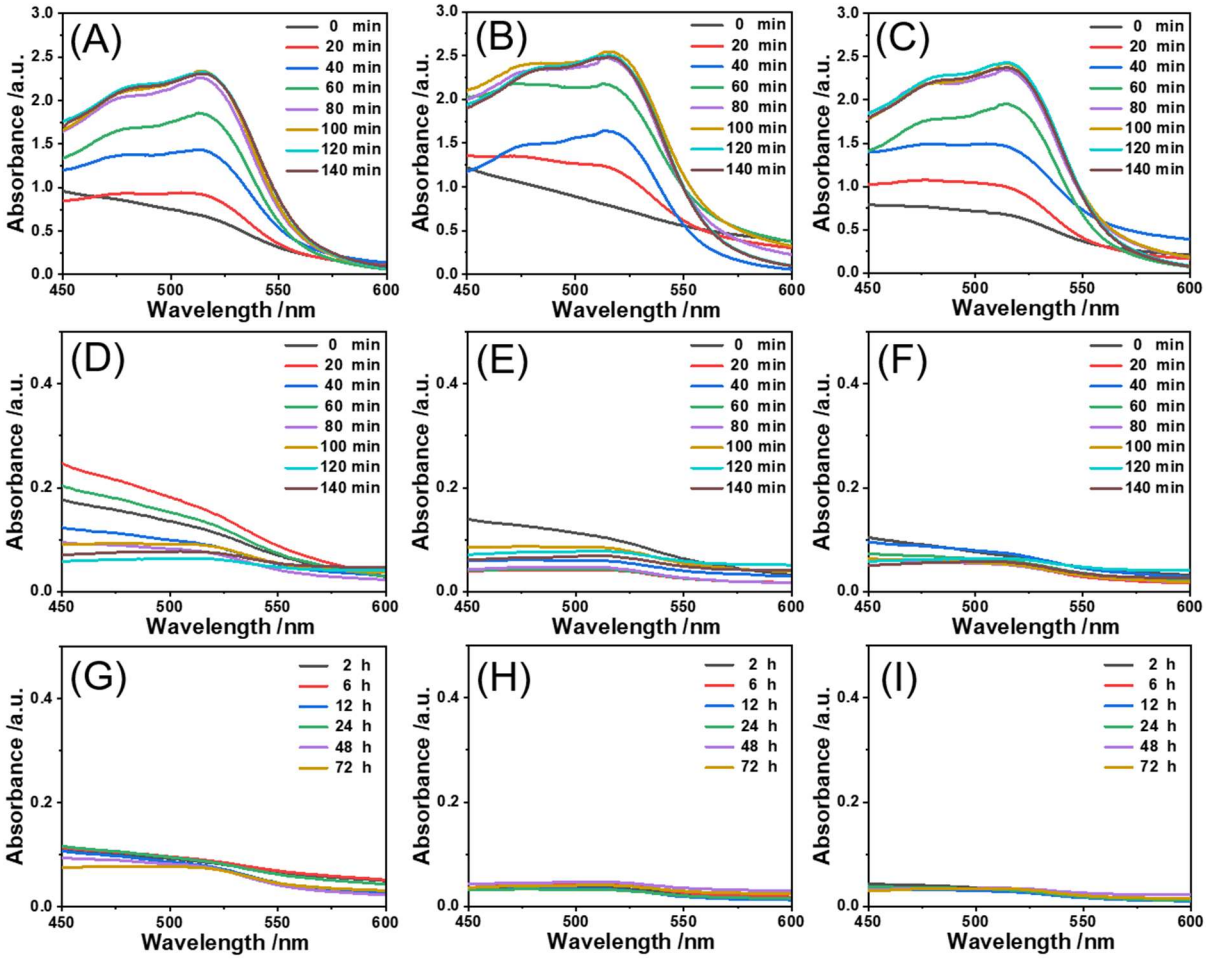

Figure S18. UV-vis spectra of the pH 2 (A), 7 (B) and 12 (C) Fe_3O_4 gels after immersed in hydrochloric acid for 140 min. UV-vis spectra of the pH 2 (D, G), 7 (E, H) and 12 (F, I) Fe_3O_4 gels after placed in deionized water for different durations. T = 25 °C.

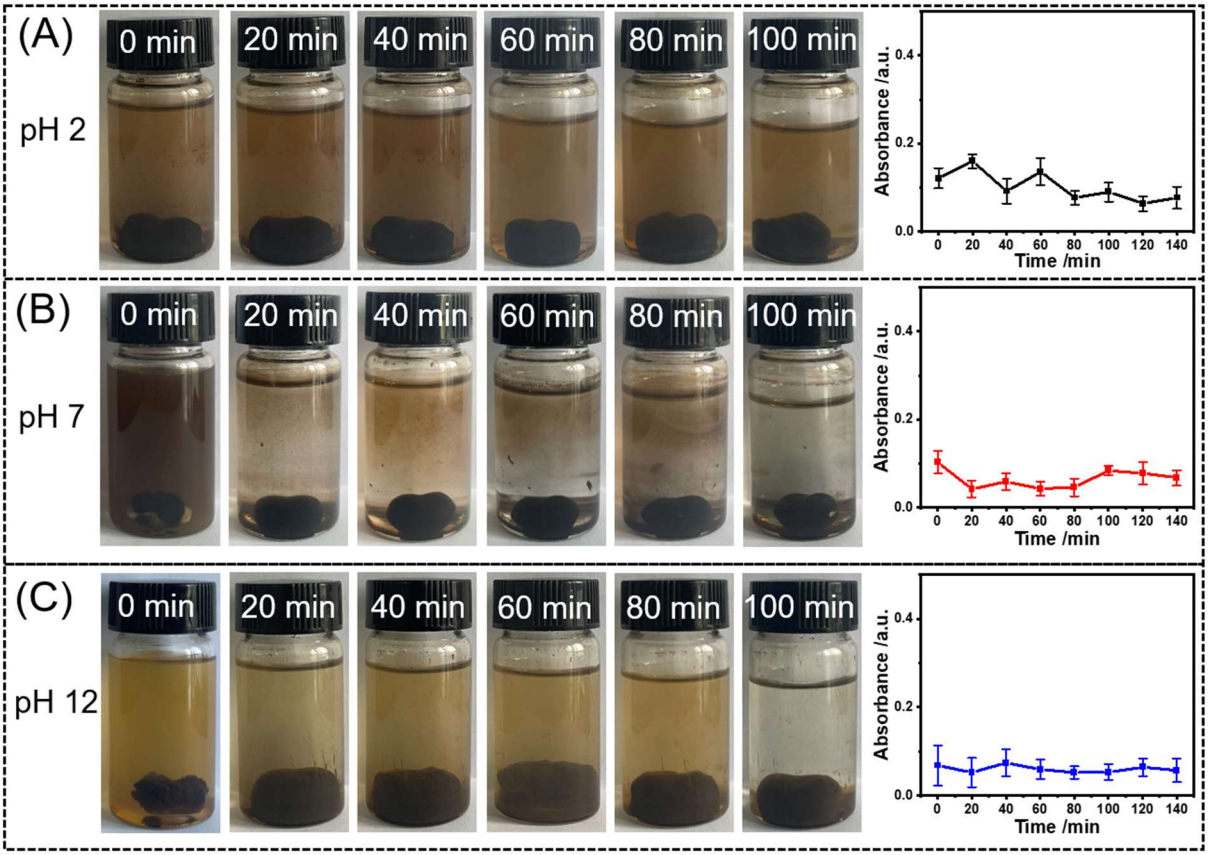

Figure S19. Variation of the pH 2 (A), 7 (B) and 12 (C) magnetic gels after placed in ultrapure water for 100 min under magnetic stirring. The UV-vis spectra on the right were used for monitoring the decomposition process by detecting the absorbance of released Fe-based ions in solutions.

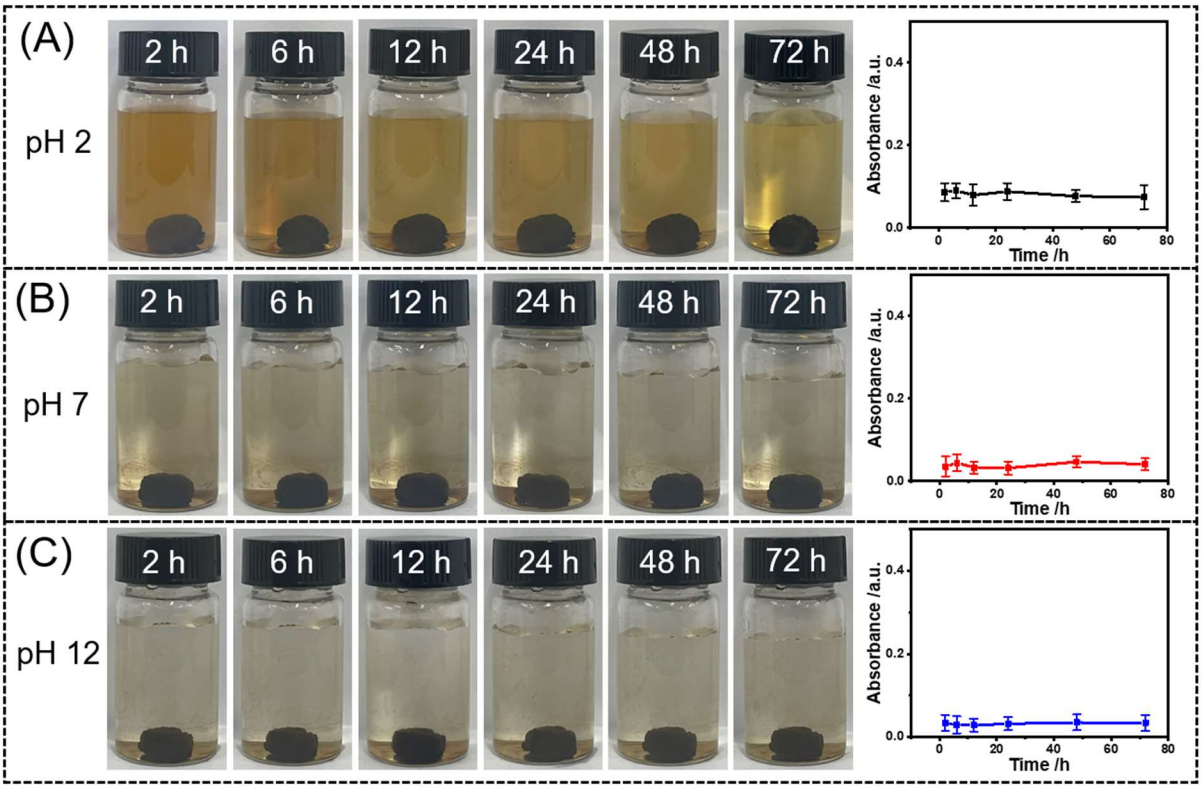

Figure S20. Variation of the pH 2 (A), 7 (B) and 12 (C) magnetic gels after placed in ultrapure water for continuous 72 h without magnetic stirring. The UV-vis spectra on the right were used for monitoring the decomposition process by detecting the absorbance of released Fe-based ions in solutions.

Figure S21. Variation of an equal amount of commercially available magnetic greases after placed in 1 mol L^{-1} HCl solutions for 100 min under magnetic stirring. The UV-vis spectra on the right were utilized to monitor the degradation process by detecting the absorbance of released Fe-based ions in solutions.

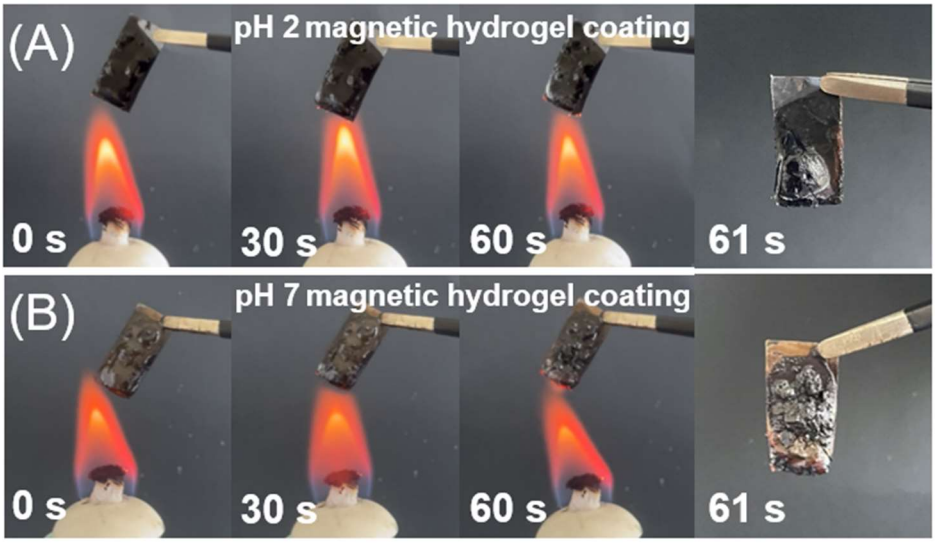

Figure S22. Photographs of plastic substrates coated with pH 2 (A) and 7 (B) Fe_3O_4 gels upon exposure to an external alcohol lamp.

Movie S1. Magnetically controlled migration of a pH 12, 48 wt% Fe_3O_4 gel by an external 0.25 T magnet at 25 °C.